Cell

Inactivation of BAD by IKK Inhibits TNFα-Induced Apoptosis Independently of NF-κB Activation

Jie Yan,[1] Jialing Xiang,[2] Yutin Lin,[2] Jingui Ma,[1] Jiyan Zhang,[1,3] Hao Zhang,[4] Jisheng Sun,[4] Nika N. Danial,[5] Jing Liu,[6] and Anning Lin[1,4,*]

[1]Ben May Department for Cancer Research, The University of Chicago, Chicago, IL 60637, USA
[2]Department of Biological and Chemical Sciences, Illinois Institute of Technology, Chicago, IL 60616, USA
[3]Department of Molecular Immunology, Institute of Basic Medical Sciences, Beijing 100850, China
[4]State Key Laboratory of Cell Biology, Institute of Biochemistry and Cell Biology, Chinese Academy of Sciences, Shanghai 200031, China
[5]Department of Cancer Biology, Dana-Farber Cancer Institute, Boston, MA 02115, USA
[6]Division of Pulmonary and Critical Care Medicine, Feinberg School of Medicine, Northwestern University, Chicago, IL 60611, USA
*Correspondence: anninglin@bsd.uchicago.edu
http://dx.doi.org/10.1016/j.cell.2012.12.021

SUMMARY

The IκB kinase complex (IKK) is a key regulator of immune responses, inflammation, cell survival, and tumorigenesis. The prosurvival function of IKK centers on activation of the transcription factor NF-κB, whose target gene products inhibit caspases and prevent prolonged JNK activation. Here, we report that inactivation of the BH3-only protein BAD by IKK independently of NF-κB activation suppresses TNFα-induced apoptosis. TNFα-treated *Ikkβ*$^{-/-}$ mouse embryonic fibroblasts (MEFs) undergo apoptosis significantly faster than MEFs deficient in both *RelA* and *cRel* due to lack of inhibition of BAD by IKK. IKK phosphorylates BAD at serine-26 (Ser26) and primes it for inactivation. Elimination of Ser26 phosphorylation promotes BAD proapoptotic activity, thereby accelerating TNFα-induced apoptosis in cultured cells and increasing mortality in animals. Our results reveal that IKK inhibits TNFα-induced apoptosis through two distinct but cooperative mechanisms: activation of the survival factor NF-κB and inactivation of the proapoptotic BH3-only BAD protein.

INTRODUCTION

The IκB kinase complex (IKK) plays a central role in immune responses, inflammation, cell survival, and tumorigenesis (Baldwin, 2012; Ghosh and Karin, 2002; Karin and Ben-Neriah, 2000; Liu et al., 2012). IKK has two catalytic subunits, IKKα and IKKβ, and two regulatory subunits, NEMO/IKKγ and ELKS (Ghosh and Karin, 2002). IKK is activated by a variety of extracellular stimuli, including inflammatory cytokines such as tumor necrosis factor (TNFα) (Baldwin, 2012; Liu et al., 2012). Once activated, IKK phosphorylates IκBs, which are a group of cytoplasmic inhibitors of NF-κB, on specific serines (Ser32 and Ser36 in IκBα and Ser19 and Ser21 in IκBβ), triggering their ubiquitination and subsequent degradation by the 26S proteasome (Karin and Ben-Neriah, 2000). This frees NF-κB dimers to translocate into the nucleus, where they stimulate transcription of the target genes involved in immune responses, inflammation, viral infection, cell survival, and tumorigenesis (Baldwin, 2012; Ghosh and Karin, 2002; Karin and Ben-Neriah, 2000; Liu et al., 2012). In addition to IκB proteins, IKK has several other substrates, including A20, BCL-10, CYLD, FOXO3a, histone H3, p85α, and RelA, which are involved in NF-κB activation or regulation of autophagy, allergy, immunity, and tumorigenesis (Anest et al., 2003; Comb et al., 2012; Hu et al., 2004; Hutti et al., 2007; Sakurai et al., 1999; Reiley et al., 2005; Wegener et al., 2006).

The prevailing paradigm of how IKK regulates TNFα-induced apoptosis is the "NF-κB activation" model, in which the target gene products of NF-κB inhibit caspases and prevent prolonged JNK activation (Karin and Lin, 2002; Liu et al., 1996, 2004; Liu and Lin, 2007; Tang et al., 2001, 2002; Wang et al., 1996a; Van Antwerp et al., 1996). Genetic disruption of RelA alleles—which are the major transactivating subunit of NF-κB in response to TNFα—in mice results in embryonic lethality with massive apoptosis of hepatocytes in the liver (Beg et al., 1995). The embryonic lethality can be rescued by inactivation of TNF receptor 1 (TNF-R1), demonstrating that RelA/NF-κB is necessary for cell survival upon TNFα stimulation (Alcamo et al., 2001). Genetic disruption of IKKβ or NEMO/IKKγ, but not IKKα, in mice severely impairs NF-κB activation induced by TNFα and other proinflammatory cytokines like IL-1, and like RelA/NF-κB deficient mice, IKKβ- or NEMO/IKKγ-deficient mice also have the embryonic lethality (Li et al., 1999a, 1999b; Rudolph et al., 2000). Although activation of NF-κB by IKK is necessary for inhibition of TNFα-induced apoptosis, it is not clear whether IKK can inhibit TNFα-induced apoptosis independently of NF-κB and, if so, what the molecular mechanism is.

The BH3-only protein BAD is a member of the proapoptotic BCL-2 family and plays a critical role in regulation of the mitochondrial death machinery by extracellular stimuli (Danial and

Korsmeyer, 2004; Danial, 2008; Dragovich et al., 1998; Youle and Strasser, 2008). In the presence of growth and survival factors, BAD is phosphorylated at the "regulatory serines" (Ser112, Ser136, and Ser155) in a sequential manner, in which phosphorylation of Ser112 and Ser136 is required for phosphorylation of Ser155 (Danial, 2008; Yaffe, 2002; Youle and Strasser, 2008). Several protein kinases, including PKA, Raf-1, Akt/PKB, Rsk2, and CaMKII, have been reported to phosphorylate BAD at one or both of these regulatory serines in response to survival signals (Bonni et al., 1999; Datta et al., 1997; del Peso et al., 1997; Harada et al., 1999; Kelekar et al., 1997; Wang et al., 1996b; Zha et al., 1996). In addition, JNK1 can phosphorylate BAD at Thr201 in response to IL-3 and thereby inhibit the proapoptotic activity of BAD (Yu et al., 2004). Upon withdrawal of survival factors, BAD is hypophosphorylated and subsequently translocates to mitochondrial membrane, where it binds to and inactivates the antiapoptotic BCL-2 family protein BCL-X_L (Danial and Korsmeyer, 2004; Danial, 2008; Youle and Strasser, 2008). However, the role of BAD in cell death induced by other death stimuli like TNFα is poorly understood. Here, we report that IKK inhibits TNFα-induced apoptosis through phosphorylation and inactivation of BAD independently of NF-κB activation. Thus, IKK inhibits TNFα-induced apoptosis through at least two distinct mechanisms: activation of the survival factor NF-κB and inhibition of the proapoptotic protein BAD.

RESULTS

IKK Is Able to Inhibit TNFα-Induced Apoptosis Independently of NF-κB Activation

We were curious whether IKK can inhibit TNFα-induced apoptosis through an NF-κB-independent mechanism. Although RelA is the major transactivating subunit of NF-κB in response to many extracellular stimuli, including TNFα, cRel has been reported to be able to compensate NF-κB activity in the absence of RelA (Barkett and Gilmore, 1999; Gerondakis et al., 1999; Grossmann et al., 1999). Thus, we used wild-type (WT), *Ikkβ*$^{-/-}$-, and *RelA*$^{-/-}$-expressing siRNA of cRel (*RelA*$^{-/-}$/sicRel) mouse embryonic fibroblasts (MEFs). TNFα-induced expression of NF-κB target genes such as IL-6 and IκBα was significantly reduced in *RelA*$^{-/-}$ MEFs and was further diminished in *RelA*$^{-/-}$/sicRel MEFs, as measured by quantitative real-time PCR analysis (Figures S1A and S1B available online) or by luciferase assays using an NF-κB reporter gene (Figure S1C). As expected, TNFα induced apoptosis in both *Ikkβ*$^{-/-}$ and *RelA*$^{-/-}$/sicRel MEFs, but not in WT fibroblasts, as measured by the cleavage of Casp-3 substrate PARP (Figure 1A). However, the rate of TNFα-induced apoptosis was significantly faster in *Ikkβ*$^{-/-}$ MEFs than that in *RelA*$^{-/-}$/sicRel MEFs; the cleavage of PARP in *Ikkβ*$^{-/-}$ MEFs almost reached to the maximum 5 hr after TNFα stimulation, compared to 9 hr in *RelA*$^{-/-}$/sicRel MEFs (Figure 1A). Similar results were obtained by Casp-3 activity assays (Figure 1B) and apoptotic cell death assays (Figure 1C), although both kinds of cells died eventually. However, this could be the result of the cell type difference. To exclude this possibility, we used the approach of siRNA silencing. Knockdown of IKKβ by its specific siRNA in *RelA*$^{-/-}$/sicRel MEFs significantly accelerated TNFα-induced apoptosis, as measured by PARP cleavage (Figure 1D), Casp-3 activation (Figure 1E), and apoptotic cell death assays (Figure 1F). By contrast, knockdown of RelA and cRel by their specific siRNAs in *Ikkβ*$^{-/-}$ MEFs had no detectable effects on TNFα-induced apoptosis (Figures 1G–1I). Similar results were obtained when IKK was knocked down in *RelA*$^{-/-}$ MEFs and RelA was knocked down in *Ikkβ*$^{-/-}$ MEFs (Figures S1D–S1G). These data demonstrate that IKK can inhibit TNFα-induced apoptosis through an NF-κB-independent mechanism.

IKK, but Not NF-κB, Suppresses BAD Proapoptotic Activity upon TNFα Stimulation

The above observation that *Ikkβ*$^{-/-}$ MEFs died significantly faster than *RelA*$^{-/-}$/sicRel MEFs suggests that, in addition to activation of NF-κB, IKK may inactivate a proapoptotic factor or activate another survival factor. To test this hypothesis, we determined whether IKK negatively regulates the BH3-only protein BAD, which is a convergent point for many survival signals (Danial and Korsmeyer, 2004; Danial, 2008; Dragovich et al., 1998; Youle and Strasser, 2008). We found that silencing of BAD by its specific siRNA significantly reduced TNFα-induced apoptosis in *Ikkβ*$^{-/-}$ MEFs, as measured by PARP cleavage (Figure 2A). Knockdown of BAD did not affect expression of BCL-X_L, which is a prosurvival BCL-2 family protein that antagonizes BAD (Figure 2A). By contrast, knockdown of BAD had no detectable effects on TNFα-induced apoptosis in *RelA*$^{-/-}$/sicRel MEFs (Figure 2B). Similar results were obtained by Casp-3 activity assays (Figure 2C). Importantly, when BAD was knocked down, *Ikkβ*$^{-/-}$ and *RelA*$^{-/-}$/sicRel MEFs had similar apoptotic rates (Figure 2C). These data indicate that the inability of inactivating BAD resulted in the higher apoptotic death rate in *Ikkβ*$^{-/-}$ MEFs (Figure 2A; see also Figures 1A–1C). When WT and *Bad*$^{-/-}$ fibroblasts were pretreated with the specific IKK inhibitor PS-1145 to block TNFα-induced activation of IKK (Figure S2A), TNFα-induced apoptosis was significantly reduced in *Bad*$^{-/-}$ MEFs compared with that in WT fibroblasts (Figure 2D). Similar results were obtained with primary hepatocytes, CHO, and FL83B cells (Figures S2C–S2E). Thus, IKK suppresses TNFα-induced apoptosis through inhibition of the proapoptotic BAD protein, in addition to activation of NF-κB in various mammalian cells.

To determine whether BAD is involved in TNFα-induced apoptosis in vivo, we used WT and *Bad* knockout mice. When D-GalN-sensitized mice were injected intraperitoneally with TNFα, WT mice had severe liver damage with massive apoptosis of hepatocytes (Figure 2E) and started to die around 6 hr (Figure 2F). By contrast, *Bad*$^{-/-}$ mice were much less sensitive to TNFα/D-GalN-induced apoptosis in liver, and the mortality was significantly reduced (Figures 2E and 2F). These results demonstrate that BAD is involved in TNFα-induced apoptosis in animals.

IKK Is a BAD Kinase

Because IKK inhibits BAD proapoptotic activity upon TNFα stimulation (Figure 2), we hypothesized that IKK may inhibit BAD through phosphorylation. Immune complex kinase assays showed that TNFα-activated IKK significantly phosphorylated purified GST-BAD fusion proteins (Figure 3A). The ability of the IKK complex to phosphorylate GST-BAD was well correlated to its phosphorylation of GST-IκBα (Figure 3A), which is an

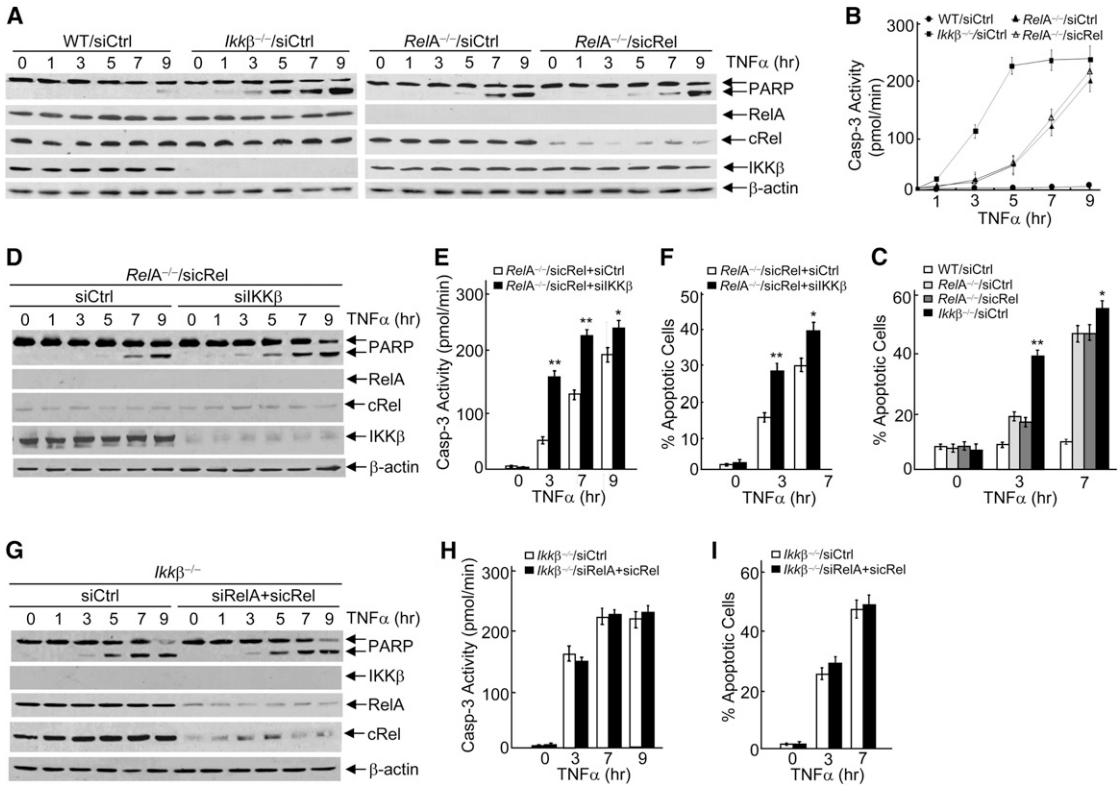

Figure 1. IKK Is Able to Inhibit TNFα-Induced Apoptosis through NF-κB-Independent Mechanism

(A–C) WT, *Ikk*β$^{-/-}$, and *RelA*$^{-/-}$ fibroblasts were transfected with siRNA against cRel (sicRel) or control siRNA (siCtrl) as indicated for 24 hr, followed by stimulation with or without TNFα (5 ng/ml). Cleavage of Casp-3 substrate PARP and expression of RelA, cRel, and IKKβ were analyzed by immunoblotting (A), measurement of Casp-3 activity (B), and apoptotic cells, which were identified by Annexin V and PI staining followed by flow cytometric analysis (C).

(D–F) *RelA*$^{-/-}$ MEFs were transfected with sicRel, along with siIKKβ or siCtrl for 24 hr, followed by stimulation with or without TNFα (5 ng/ml). PARP cleavage and expression of IKKβ and cRel were analyzed (D). Casp-3 activity (E) and apoptotic cell death (F) were measured as described in (B) and (C), respectively.

(G–I) *Ikk*β$^{-/-}$ MEFs were transfected with siRelA plus sicRel or siCtrl for 24 hr, followed by stimulation with or without TNFα (5 ng/ml). PARP cleavage and expression of RelA and cRel were analyzed (G). Casp-3 activity (H) and apoptotic cell death (I) were measured as in (B) and (C), respectively.

The results in (B), (C), (E), (F), (H), and (I) are presented as means ±SE and represent three individual experiments. *$p < 0.05$ and **$p < 0.01$, as analyzed by Student's t test. See also Figure S1.

authentic IKK substrate. Knockout of IKKβ, which is responsible for suppressing TNFα-induced apoptosis (Ghosh and Karin, 2002), almost completely abolished phosphorylation of GST-BAD by TNFα-activated IKK, whereas ectopic expression of IKKβ in *Ikk*β$^{-/-}$ MEFs restored the ability of IKK to phosphorylate GST-BAD (Figure 3B). Thus, IKKβ is not only required for activation of NF-κB but is also involved in phosphorylation of the pro-apoptotic BAD protein upon TNFα stimulation.

To determine whether IKKβ can directly phosphorylate BAD, we used constitutively active IKKβ(EE), in which Ser177 and Ser181 were replaced by glutamic acids (Mercurio et al., 1997; Zandi et al., 1997). In vitro kinase assays showed that purified IKKβ(EE) significantly phosphorylated GST-BAD, as well as GST-IκBα, but not JNK substrate GST-c-Jun (Figure 3C). Two-dimensional tryptic phosphopeptide mapping revealed that GST-BAD phosphorylated by IKK isolated from nonstimulated fibroblasts (basal IKK) contained two phosphopeptides, *a* and *b* (Figure 3D). When GST-BAD phosphorylated by TNFα-activated IKK was analyzed, the phosphopeptide *a* was significantly increased, whereas the phosphopeptide *b* remained unchanged, with the appearance of another minor phosphopeptide *c* (Figure 3D). This suggests that phosphopeptide *a*, as well as phosphopeptide *c*, to a much less extent, were specifically phosphorylated by active IKK. Similar results were obtained when IKKβ(EE)-phosphorylated GST-BAD was analyzed (Figure 3D). Phosphoamino acid analysis revealed that GST-BAD phosphorylated by active IKK, as well as the phosphopeptide *a*, only contained phosphoserine (PS) (Figure 3E). Taken together, these results demonstrate that IKKβ is a BAD kinase that phosphorylates BAD at serine residue(s).

IKK Is Necessary and Sufficient to Phosphorylate BAD at Ser26 In Vitro and In Vivo

To identify IKK-phosphorylated serine residue(s), we constructed a C-terminal truncated GST-ΔC-BAD(1–114) and an N-terminal truncated GST-ΔN-BAD(115–204) (Figure S3A). Immune complex kinase assays showed that GST-ΔN-BAD(115–204) was phosphorylated by basal IKK, and the phosphorylation was only slightly increased when active IKK was used (Figure S3A). By contrast, phosphorylation of GST-ΔC-BAD(1–114) was significantly enhanced when TNFα-activated IKK was used

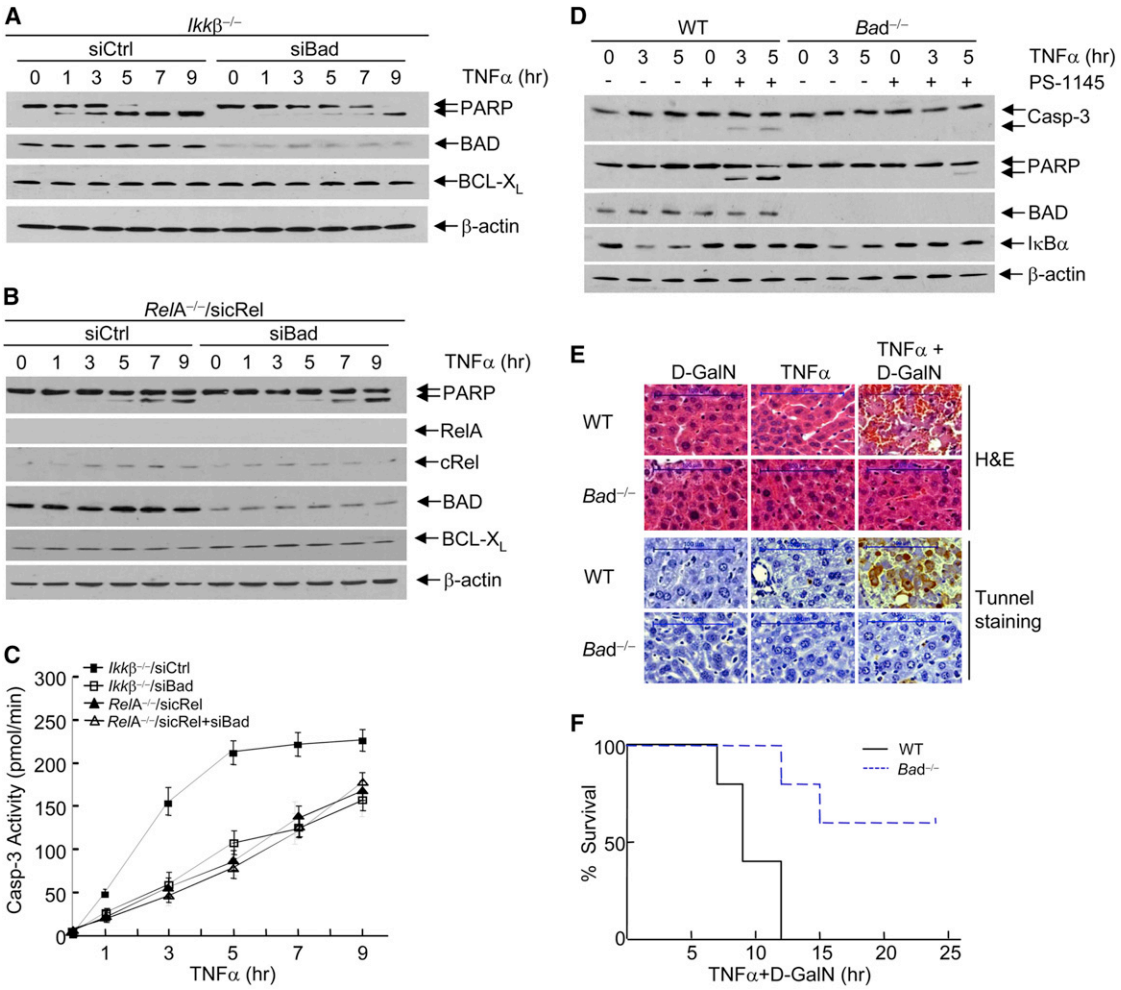

Figure 2. IKK, but Not NF-κB, Suppresses BAD Proapoptotic Activity upon TNFα Stimulation

(A–C) *Ikkβ*$^{-/-}$ or *RelA*$^{-/-}$ MEFs were transfected with siBad, sicRel, or siCtrl as indicated for 24 hr, followed by stimulation with or without TNFα (5 ng/ml). PARP cleavage and expression levels of RelA, cRel, BAD, BCL-X_L, and β-actin (A and B), as well as Casp-3 activity (C), were determined.

(D) WT and *Bad*$^{-/-}$ MEFs were pretreated with or without the specific IKKβ inhibitor PS-1145 (10 μM) for 2 hr, followed by stimulation with or without TNFα (5 ng/ml). Cleavage of pro-Casp-3 and PARP and expression levels of BAD, IκBα, and β-actin were determined. The data in (A)–(D) represent two to three individual experiments with similar results.

(E and F) WT and *Bad*$^{-/-}$ mice were sensitized with D-GalN and then treated with TNFα (see Experimental Procedures for details). Dying animals were premoved, and the livers were extracted for H&E staining and Tunnel staining (E). Mortality rate was determined, $p < 0.05$; $n = 5$ (F), as analyzed by the log rank (Mantel-Cox) test. See also Figure S2.

(Figure S3A). Two-dimensional phosphopeptide mapping analysis revealed that, in comparison to GST-BAD, GST-ΔN-BAD contained phosphopeptide *b*, whereas GST-ΔC-BAD contained phosphopeptide *a* (major) and *c* (minor) (Figure S3B). These results indicate that active IKK phosphorylation site(s) are located in the N-terminal half of BAD.

To determine the precise IKK-phosphorylation site(s) on BAD, we systemically replaced all serine residues within the N-terminal half (1–114) in the full-length GST-BAD with nonphosphorylatable alanines either individually or in different combinations, using a site-directed mutagenesis approach (Figure S3C). Immune complex kinase assays showed that TNFα-activated IKK was unable to phosphorylate the GST-BAD(S26A) mutant in comparison to WT GST-BAD (Figure 4A). Similar results were obtained with purified IKKβ(EE) (Figure 4B). By contrast, other GST-BAD mutants were still phosphorylated by active IKK (Figure S3D). Two-dimensional phosphopeptide mapping revealed that the replacement of Ser26 by Ala resulted in complete elimination of the phosphopeptide *a* and *c* but had no effects on phosphopeptide *b* (Figure 4C). Analysis of IKK-phosphorylated GST-BAD proteins by tandem mass spectrometry (MS/MS) also revealed that Ser26 was phosphorylated by IKK (Figure 4D).

To analyze the regulation of BAD Ser26 phosphorylation in vivo, we generated a rabbit polyclonal antibody using a synthetic BAD phosphopeptide containing phosphorylated Ser26 as an immunogen. Immunoblotting analysis revealed that the anti-phospho-Ser26 antibody specifically recognized

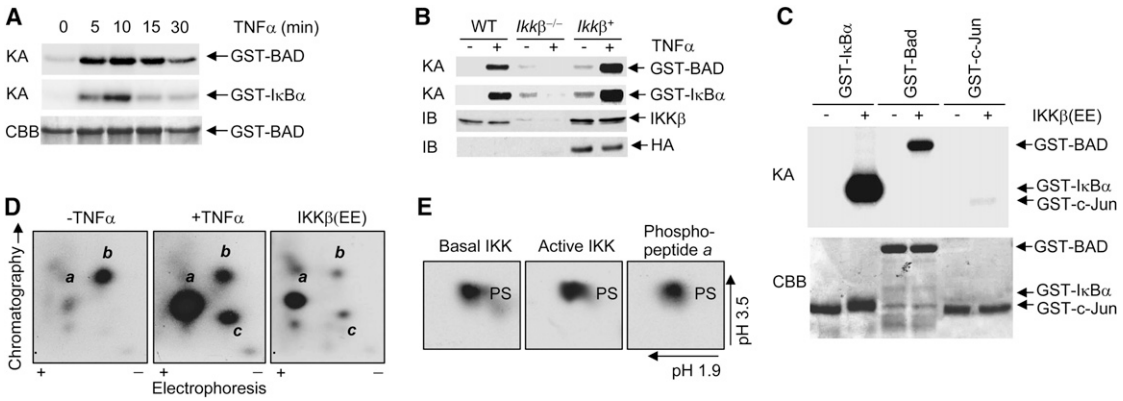

Figure 3. IKK Is a BAD Kinase

(A) WT MEFs were stimulated with or without TNFα (5 ng/ml). IKK activity was determined by immune complex kinase assays with purified GST-IκBα (5 μg) or GST-BAD (5 μg) as substrate. CBB, Coomassie brilliant blue staining.

(B) WT, *Ikkβ*$^{-/-}$, and *Ikkβ*$^{+}$ MEFs, in which *Ikkβ*$^{-/-}$ MEFs were infected with adenoviral vector-encoding HA-IKKβ (300 MOI; 24 hr), were stimulated with or without TNFα (5 ng/ml) for 10 min. IKK activity was determined as in (A).

(C) In vitro phosphorylation of purified GST-IκBα, GST-BAD, and GST-c-Jun (5 μg each) by constitutively active IKKβ(EE) (24 ng), in which Ser177 and Ser181 were replaced by glutamic acids (EE) and has been purified to near homogeneity.

(D) Phosphorylated GST-BAD proteins were subjected to two-dimensional tryptic phosphopeptide mapping as described (Lin et al., 1992). Spot *b* is the major tryptic peptide phosphorylated by basal IKK; spots *a* and *c* represent the peptides whose phosphorylation was augmented by active IKK or IKKβ(EE).

(E) Phosphorylated BAD or the phosphopeptide *a* was subjected to phosphoamino acid analysis as described (Lin et al., 1992). PS, phosphoserine.

The data in (A)–(C) represent two to three individual experiments with similar results.

active IKK-phosphorylated GST-BAD, but not nonphosphorylated GST-BAD or GST-BAD(S26A) mutant (Figure 4E). This was not a result of the difference in the amount of GST-BAD proteins, as analyzed by immunoblotting using anti-GST antibody (Figure 4E). Thus, anti-phospho-Ser26 antibody specifically recognizes BAD when it is phosphorylated at Ser26 by IKK.

To determine whether BAD is phosphorylated at Ser26 in response to TNFα in an IKK-dependent manner, we used *Ikkβ*$^{-/-}$ MEFs. Immunoblotting analysis using anti-phospho-Ser26 antibody revealed that TNFα rapidly induced BAD phosphorylation at Ser26 in WT, but not in *Ikkβ*$^{-/-}$ MEFs (Figure 4F). Consistently, ectopic expression of WT IKKβ in *Ikkβ*$^{-/-}$ MEFs restored BAD phosphorylation at Ser26 in response to TNFα stimulation (Figure 4G). Furthermore, ectopic expression of the constitutively active IKKβ(EE) alone was sufficient to induce BAD phosphorylation at Ser26 (Figure 4G). Interestingly, BAD was also slightly phosphorylated at Ser26 in resting WT fibroblasts (Figure S3E, longer exposure). This basal level phosphorylation of BAD at Ser26 was completely diminished in *Ikkβ*$^{-/-}$ MEFs (Figure S3E, longer exposure), suggesting that IKK is also responsible for BAD basal Ser26 phosphorylation. Taken together, IKK is necessary and sufficient for BAD phosphorylation at Ser26 under both basal and stimulated conditions.

IKK Inhibits the Association between BAD and BCL-X_L Independently of NF-κB Activation

We hypothesized that phosphorylation by IKK may promote BAD interaction with 14-3-3, thereby preventing BAD from translocating to the mitochondria to inactivate BCL-X_L. To test this idea, we examined the effect of IKKβ on the subcellular localization of BAD. TNFα induced apoptotic cell death in *Ikkβ*$^{-/-}$, but not in WT fibroblasts, as previously reported (Tang et al., 2001; see also Figure 1). Immunoblotting analysis revealed that BAD and Ser26-phosphorylated BAD exclusively localized in the cytosolic fractions in TNFα-treated WT fibroblasts (Figure 5A). By contrast, a small portion (~3%–6%) of the cytoplasmic BAD, which was not phosphorylated at Ser26, translocated to the mitochondria in TNFα-treated *Ikkβ*$^{-/-}$ MEFs (Figure 5A). In fact, a small portion of the cytoplasmic BAD started to translocate to mitochondria as early as 5 min after TNFα stimulation in *Ikkβ*$^{-/-}$ MEFs (Figure S4A). These results suggest that IKKβ may inhibit mitochondrial translocation of BAD. However, it is possible that translocation of BAD to the mitochondria is the consequence of TNFα-induced apoptosis in *Ikkβ*$^{-/-}$ MEFs. To exclude this possibility, we determined the effect of IKKβ on the interaction between BAD and 14-3-3 or BCL-X_L. We found that BAD, as well as Ser26-phosphorylated BAD, interacted with 14-3-3 in the cytosol in TNFα-treated WT, but not in *Ikkβ*$^{-/-}$ fibroblasts (Figure 5B). Although total cytosolic Ser26-phosphorylated BAD was reduced with time, 14-3-3-associated Ser26-phosphorylated BAD remained unchanged even 3 hr after TNFα stimulation, suggesting that binding with 14-3-3 may inhibit dephosphorylation of Ser26-phosphorylated BAD. Conversely, BCL-X_L interacted with BAD in the mitochondrial fractions of TNFα-treated *Ikkβ*$^{-/-}$, but not WT fibroblasts (Figure 5C). More importantly, only nonphosphorylated, but not Ser26-phosphorylated, BAD was found to associate with BCL-X_L at the mitochondria (Figure 5C). Immunoprecipitation of BAD from the mitochondria fraction of TNFα-treated *Ikkβ*$^{-/-}$ MEFs also showed that there was no Ser26-phosphorylated BAD (Figure S4B). Taken together, these data demonstrate that phosphorylation of BAD by IKK at Ser26 prevents BAD from translocating to the mitochondria to bind to and inactivate BCL-X_L, thereby inhibiting the proapoptotic activity of BAD upon TNFα stimulation.

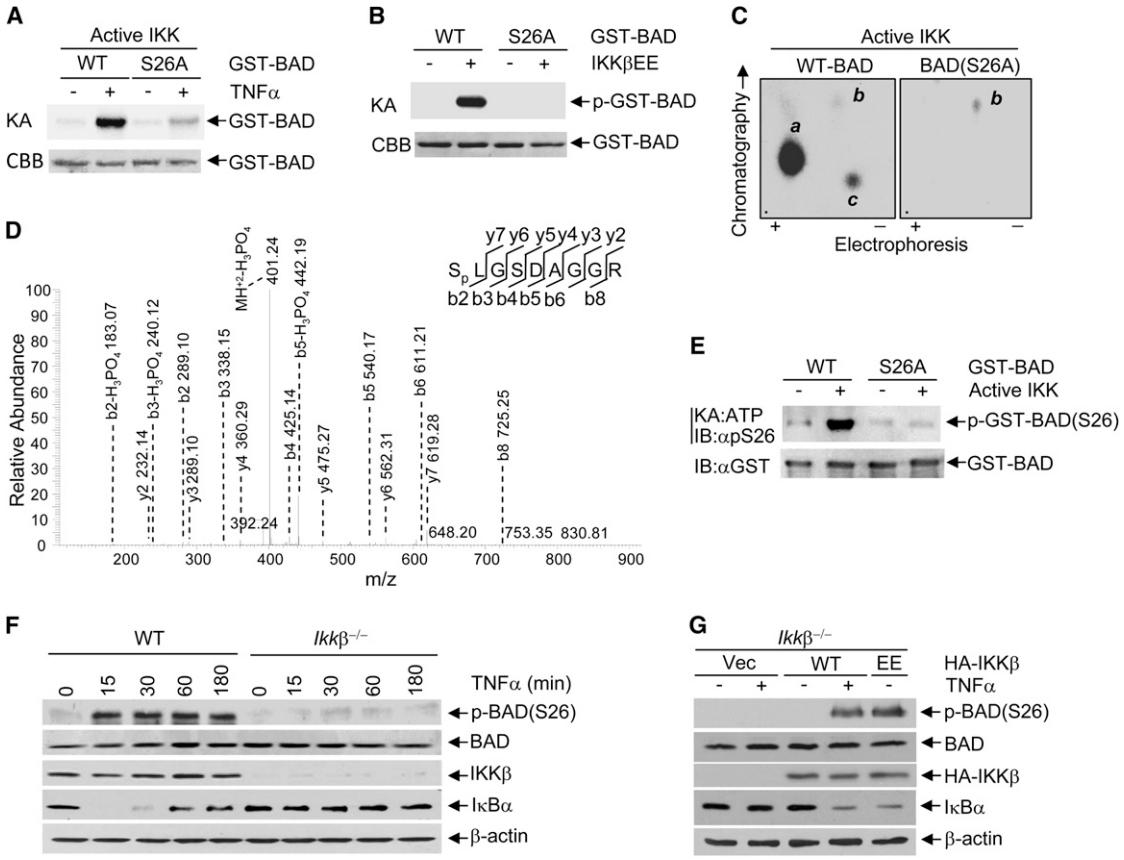

Figure 4. IKK Is Necessary and Sufficient to Phosphorylate BAD at Ser26 In Vitro and In Vivo

(A and B) Phosphorylation of GST-BAD and GST-BAD(S26A) mutant proteins by active IKK (A) or purified IKKβ(EE) proteins (B), as described in Figure 3B.

(C) Two-dimensional phosphopeptide mapping of active IKK-phosphorylated GST-BAD and GST-BAD(S26A) mutant proteins, as described in Figure 3D.

(D) GST-BAD proteins phosphorylated by active IKK in vitro were tryptic digested and then analyzed by mass spectrometry. Insert shows the recovered phosphorylated peptide fragment corresponding to S26.

(E) GST-BAD and GST-BAD(S26A) proteins were phosphorylated by active IKK in the presence of nonradioactive ATP (17 μM) and analyzed by immunoblotting using anti-phospho-Ser26 antibody.

(F) WT and *Ikkβ*$^{-/-}$ MEFs were stimulated with or without TNFα (5 ng/ml). Ser26-phosphorylation of BAD and expression levels of BAD, IKKβ, IκBα, and β-actin were determined.

(G) *Ikkβ*$^{-/-}$ MEFs were transfected with WT HA-IKK, constitutive active HA-IKKβ(EE), or empty vector (1 μg each), followed by stimulation with or without TNFα (5 ng/ml, 10 min). Ser26-phosphorylation of BAD and expression levels of HA-IKKβ, HA-IKKβ(EE), and IκBα were determined.

The data in (A), (B), and (E)–(G) represent two to three individual experiments with similar results. See also Figure S3.

To determine whether inhibition of TNFα-induced BAD mitochondrial translocation by IKK is independent of NF-κB activation, we used *RelA*$^{-/-}$ MEFs. We found that BAD, as well as Ser26-phosphorylated BAD, associated with 14-3-3 in the cytosolic fractions in both TNFα-treated WT and *RelA*$^{-/-}$ MEFs, but not in *Ikkβ*$^{-/-}$ MEFs (Figure 5D). Consistently, BAD only associated with BCL-X_L in the mitochondrial fractions of TNFα-treated *Ikkβ*$^{-/-}$ MEFs, but not WT and *RelA*$^{-/-}$ MEFs (Figure 5E). These data demonstrate that inhibition of BAD by IKK is independent of its activation of NF-κB.

IKK Primes BAD for Its Phosphorylation at the Regulatory Serines

To understand how IKK inhibits BAD mitochondria translocation, we determined its effect on BAD phosphorylation at the regulatory serines. Immunoblotting analysis revealed that phosphorylation of the regulatory serines (Ser112, Ser136, and Ser155) was impaired in *Ikkβ*$^{-/-}$ MEFs upon TNFα stimulation (Figure 6A). This result suggests that IKK may prime BAD for its phosphorylation at the regulatory serines, thereby regulating BAD mitochondria translocation.

To determine whether inhibition of BAD mitochondria translocation by IKK indeed depends on priming BAD phosphorylation at the regulatory serines, *Bad*$^{-/-}$ MEFs stably expressing HA-BCL-X_L were transiently transfected with M2-Bad WT [*Bad*(WT)$^{+}$] or M2-Bad(3SA) mutant, in which Ser112, Ser136, and Ser155 were replaced by alanines [*Bad*(3SA)$^{+}$] (Figure 6B). Although BAD(3SA) mutant could not be phosphorylated at the regulatory serines, it was still phosphorylated at Ser26 upon TNFα stimulation (Figure 6B). Under the same conditions, a small

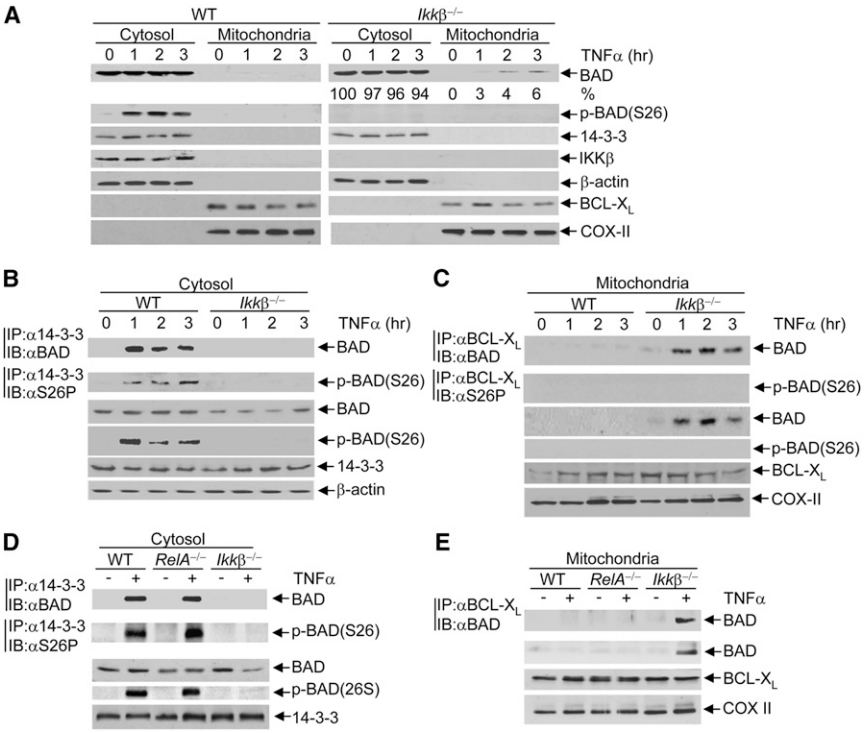

Figure 5. Phosphorylation of BAD by IKKβ Inhibits Its Proapoptotic Activity

(A) WT and *Ikkβ*$^{-/-}$ MEFs were treated with or without TNFα (5 ng/ml) and then separated into cytosol and mitochondrial fractions. Subcellular localization of BAD, Ser26-phosphorylated BAD, 14-3-3, BCL-X_L, and IKKβ was analyzed by immunoblotting. β-actin and COX-II were used as cytosol and mitochondrial markers, respectively. The amount of BAD in cytosol and mitochondrial fractions in the same numbers of *Ikkβ*$^{-/-}$ MEFs were quantitated by the Image J program.

(B and C) WT and *Ikkβ*$^{-/-}$ MEFs were treated with or without TNFα (5 ng/ml) and fractionated as described in (A). 14-3-3- and BCL-X_L-associated BAD or Ser26-phosphorylated BAD were analyzed by immunoprecipitation in combination with immunoblotting. BAD Ser26-phosphorylation, expression levels of BAD, 14-3-3, BCL-X_L, β-actin, and COX-II were determined.

(D and E) WT, *RelA*$^{-/-}$, and *Ikkβ*$^{-/-}$ MEFs were stimulated with or without TNFα (5 ng/ml, 1 hr) and then separated into cytosol (D) and mitochondria (E) fractions. 14-3-3- and BCL-X_L-associated BAD or Ser26-phosphorylated BAD, BAD Ser26-phosphorylation, expression levels of BAD, 14-3-3, BCL-X_L, and COX-II were determined as described in (B) and (C).

All data represent two to three individual experiments with similar results. See also Figure S4.

portion of BAD(3SA) mutant (~3%–7%), but not WT BAD, translocated to the mitochondria (Figure 6C). Importantly, a similar portion of Ser26-phosphorylated BAD(3SA) mutant (~3%–6%) also translocated to the mitochondria translocation (Figure 6C). Furthermore, apoptotic cell death was significantly increased in TNFα-treated *Bad*(3SA)$^+$ MEFs in comparison with *Bad*(WT)$^+$ MEFs (Figure 6D). Taken together, the inhibition of BAD mitochondria translocation and proapoptotic activity by IKK indeed depends on priming BAD phosphorylation at the regulatory serines.

To determine whether priming BAD phosphorylation at the regulatory serines by IKK is involved in suppression of TNFα-induced apoptosis in vivo, we used WT and *Bad*$^{3SA/3SA}$ knockin mice. Immunoblotting analysis revealed that the expression level of BAD(3SA) mutant was similar to that of endogenous BAD (Figure S5A). When D-GalN-sensitized mice were injected intraperitoneally with TNFα, *Bad*$^{3SA/3SA}$ knockin mice had accelerated and severe liver damage with massive hepatocyte apoptosis and mortality as compared to WT mice (Figures S5B and 6E). These results suggest that priming BAD phosphorylation by IKK at the regulatory serines is required for suppression of TNFα-induced apoptosis in vivo.

Phosphorylation of BAD at Ser26 by IKK Inhibits the Proapoptotic Activity of BAD

To determine the role of IKK-mediated Ser26 phosphorylation in regulation of BAD proapoptotic activity, we established *Bad*$^{-/-}$ stable cell lines expressing similar levels of WT M2-BAD or M2-BAD(S26A) mutant (Figure S6A). As expected, immunoblotting analysis revealed that ectopically expressed WT BAD, but not BAD(S26A) mutant, was phosphorylated at Ser26 upon TNFα stimulation (Figure S6A). In addition, TNFα induced phosphorylation of WT BAD, but not BAD(S26A) mutant at Ser112, Ser136, and Ser155 (Figure S6A). Furthermore, there were no detectable differences in TNFα-induced activation of IKK and NF-κB between *Bad*(WT)$^+$ and *Bad*(S26A)$^+$ MEFs, as measured by IκBα degradation and resynthesis (Figure S6A) and by the promoter activity of NF-κB by luciferase assays (Figure S6B). These results demonstrate that elimination of IKK-mediated Ser26-phosphorylation abrogates BAD phosphorylation at the regulatory serines without affecting IKK activity and NF-κB activation upon TNFα stimulation.

Next, we determined whether IKK-mediated Ser26 phosphorylation of BAD is required for suppression of TNFα-induced apoptosis. TNFα induced apoptosis in both *Bad*(WT)$^+$ and *Bad*(S26A)$^+$ MEFs when cells were infected with adenoviral vector encoding HA-IκBα(AA) (Figure 7A). However, like *Ikkβ*$^{-/-}$ MEFs (Figure 1A) and *Bad*(3SA)$^+$ MEFs (Figure 6D), *Bad*(S26A)$^+$ MEFs were significantly more sensitive to TNFα-induced apoptosis than *Bad*(WT)$^+$ MEFs; PARP cleavage was detected as early as 1 hr after TNFα stimulation in *Bad*(S26A)$^+$ MEFs but was detected 3 hr after in *Bad*(WT)$^+$ MEFs (Figure 7A). Apoptotic cell death assays also showed that *Bad*(S26A)$^+$ MEFs died significantly faster than *Bad*(WT)$^+$ MEFs (Figure 7B). The difference in the apoptotic death rate between *Bad*(WT)$^+$ and *Bad*(S26A)$^+$ MEFs mirrored the kinetic difference of TNFα-induced apoptosis between *RelA*$^{-/-}$ and *Ikkβ*$^{-/-}$ MEFs (Figure 1C). Similar results were obtained when Casp-3 activity

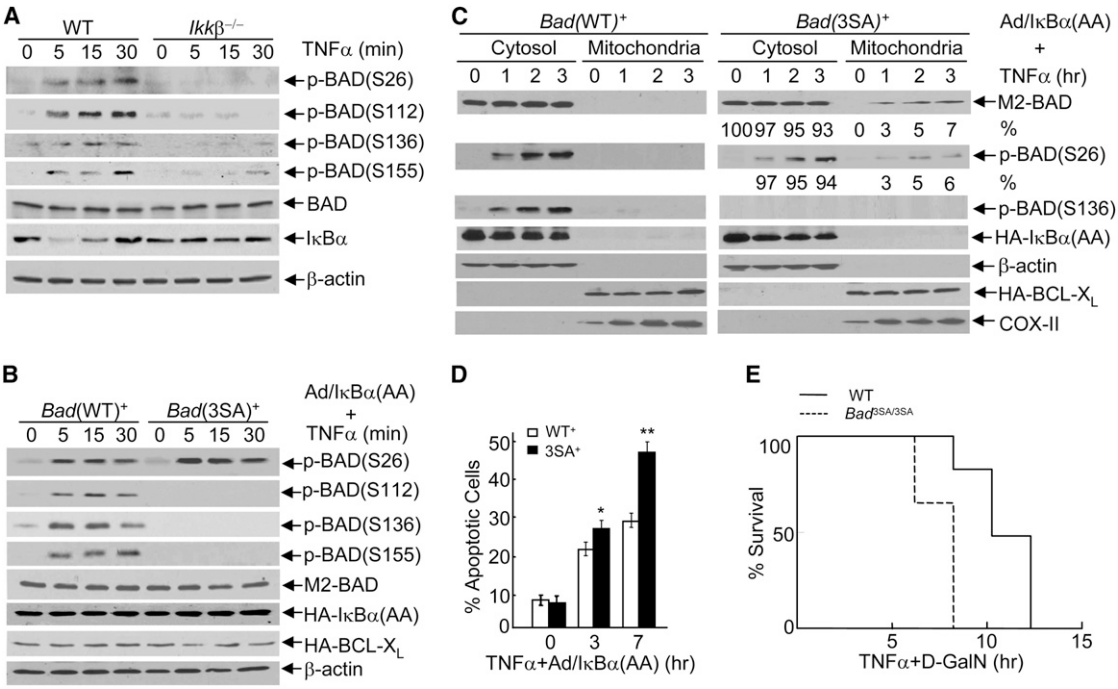

Figure 6. IKK Primes BAD Phosphorylation at the Regulatory Serines

(A) WT and *Ikkβ*$^{-/-}$ MEFs were treated with or without TNFα (5 ng/ml). Phosphorylation of BAD at various serines (Ser26, Ser112, Ser136, and Ser155) and expression levels of BAD, IκBα, and β-actin were analyzed by immunoblotting.

(B–D) *Bad*$^{-/-}$ MEFs stably expressing HA-BCL-X_L were transfected with WT M2-Bad [*Bad*(WT)$^+$] or M2-Bad(3SA) mutant, in which Ser112, Ser136, and Ser155 were replaced by analines [*Bad*(3SA)$^+$] and then infected with adenoviral vector encoding HA-IκBα(AA), in which Ser32 and Ser36 were replaced by alanines, for 24 hr. Cells were treated with or without TNFα (5 ng/ml) and either directly harvested (B) or further separated into cytosol and mitochondria fractions (C). Phosphorylation of Ser26 and the regulatory serines and expression levels of M2-BAD, HA-IκBα(AA), HA-BCL-X_L, and β-actin were determined (B and C). At each time point, the sum of cytoplasmic and mitochondrial Ser26-phosphorylated BAD(3SA) was calculated as 100% (C). The data in (A)–(C) represent two to three individual experiments with similar results. Apoptotic cell death was determined (D). The results are presented as means ±SE and represent three individual experiments. *$p < 0.05$ and **$p < 0.01$, as analyzed by Student's t test.

(E) WT and *Bad*$^{3SA/3SA}$ knockin mice were sensitized by D-GalN and then injected intraperitoneally with TNFα, as described in Figures 2E and 2F. Dying animals were premoved, and mortality rate was determined, $p < 0.001$; $n = 6$ (E), as analyzed by log rank (Mantel-Cox) test.

See also Figure S5.

was measured (Figure 7C). Under the same conditions, TNFα induced phosphorylation of the regulatory serine residues (Ser112, Ser136, and Ser155) in *Bad*(WT)$^+$, but not in *Bad*(S26A)$^+$ MEFs (Figure 7D), suggesting that elimination of Ser26 phosphorylation promotes BAD proapoptotic activity.

To determine whether IKK-mediated Ser26-phosphorylation of BAD is involved in TNFα-induced apoptosis in vivo, we used WT and *Bad* knockout mice that have been reconstituted with WT *Bad* or *Bad*(S26A) mutant via adenovirus infection. Immunoblotting analysis revealed that expression levels of reconstituted BAD were similar to that of endogenous BAD (Figure S6C). When D-GalN-sensitized mice were injected intraperitoneally with TNFα, WT mice infected with Ad/Ctrl [WT+Ad/Ctrl] and *Bad*$^{-/-}$ mice infected with Ad/WT *Bad* [*Bad*(WT)$^+$] had similar levels of liver damage and apoptosis of hepatocytes (Figure S6D), and both died within 14 hr (Figure 7E), whereas *Bad*$^{-/-}$ mice infected with Ad/Ctrl were much less sensitive to TNFα/D-GalN-induced apoptosis in liver with significantly reduced mortality (Figure 7E), which is consistent with the results in Figure 2F. By contrast, *Bad*$^{-/-}$ mice infected with Ad/*Bad*(S26A) mutant [*Bad*(S26A)$^+$] had accelerated and severe liver damage with massive apoptosis of hepatocytes (Figure S6D) and died within 10 hr (Figure 7E). Taken together, these results demonstrate that IKK-mediated Ser26-phosphorylation of BAD is required for suppression of TNFα-induced apoptosis in vivo.

DISCUSSION

It has long been thought that IKK inhibits TNFα-induced apoptosis through activation of NF-κB (Baldwin, 2012; Ghosh and Karin, 2002; Karin and Ben-Neriah, 2000; Karin and Lin, 2002; Liu and Lin, 2007). Overwhelming evidence shows that IKKβ is essential for TNFα to activate NF-κB, which in turn inhibits TNFα-induced apoptosis (Baldwin, 2012; Hoffmann and Baltimore, 2006; Karin and Lin, 2002; Liu and Lin, 2007). Although several IKK substrates, including p53, FOXO3a, TSC-1, IRS-1, and Dok-1, are involved in cell survival related to allergy, immunity, and cancer (Baldwin, 2012), their role in IKK-mediated inhibition of TNFα-induced apoptosis remains obscure. In this report, we demonstrate that phosphorylation and inactivation of BAD by

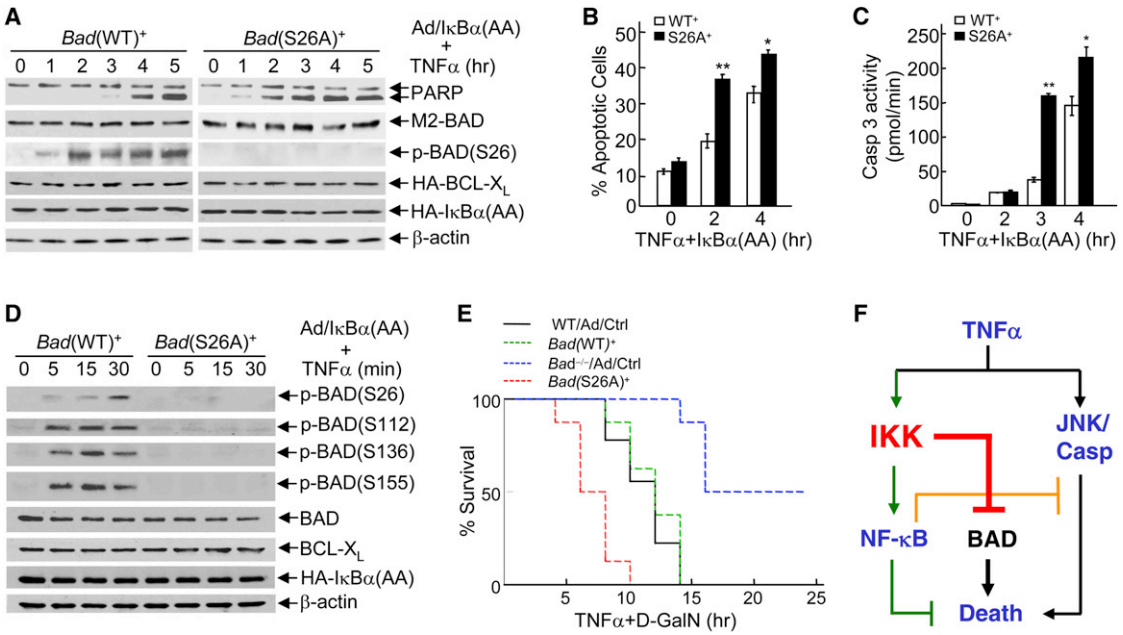

Figure 7. Elimination of Ser26-Phosphorylation Promotes the Proapoptotic Activity of BAD In Vitro and In Vivo

Bad$^{-/-}$ MEFs stably expressing WT M2-Bad [*Bad*(WT)$^+$] or M2-BAD(S26A) mutant [*Bad*(S26A)$^+$] along with HA-BCL-X_L were established as described in Experimental Procedures.

(A–D) *Bad*(WT)$^+$ and *Bad*(S26A)$^+$ MEFs were infected with adenoviral vector encoding HA-IκBα(AA) for 24 hr and then treated with or without TNFα (5 ng/ml) as indicated. PARP cleavage, expression of M2-BAD, HA-BCL-X_L, HA-IκBα(AA), β-actin, and Ser26-phosphorylation of M2-BAD were analyzed (A). Apoptotic cell death was analyzed by Annexin V/PI staining, followed by flow cytometric analysis (B), and Casp-3 activity was determined (C). The results in (B) and (C) are presented as means ±SE and represent three individual experiments. *$p < 0.05$ and **$p < 0.01$, as analyzed by Student's t test. Phosphorylation of M2-BAD at various serine residues (Ser26, Ser112, Ser136, and Ser155) and expression levels of M2-BAD, HA-BCL-X_L, HA-IκBα(AA), and β-actin were analyzed by immunoblotting (D). The data in (A)–(D) represent two to three individual experiments with similar results.

(E) *Bad*$^{-/-}$ mice were injected intravenously with Ad/WT *Bad*, Ad/*Bad*(3SA) mutant, or Ad/Ctrl (see Experimental Procedures for details) and then challenged with TNFα and D-GalN, as described in Figures 2E and 2F. Mortality rate was determined, $p < 0.001$; n = 10 (E), as analyzed by log rank (Mantel-Cox) test.

(F) A schematic presentation of the mechanism by which IKK inhibits TNFα-induced apoptosis through activation of NF-κB and inhibition of BAD.

See also Figure S6.

IKK independently of NF-κB is required for suppressing TNFα-induced apoptosis. Thus, IKK inhibits TNFα-induced apoptosis through at least two distinct mechanisms: activation of NF-κB and inhibition of BAD (Figure 7F).

Our finding that TNFα via IKK inhibits the proapoptotic activity of BAD unmasks the involvement of a mitochondria-dependent death pathway in TNFα-induced apoptosis. TNFα-induced apoptosis is mainly mediated by the receptor-dependent death pathway (Baud and Karin, 2001). Our results show that BAD was involved in TNFα-induced apoptosis in various cultured cells (fibroblasts, CHO, FL83B, and primary thymocytes and hepatocytes) (Figures 2D and S2C–S2E) and in animals (Figures 2E and 2F). Thus, TNFα can induce apoptosis through both receptor-dependent death pathway and BAD-dependent mitochondrial death pathway.

IKK is a BAD kinase upon TNFα stimulation. The proapoptotic activity of BAD is inhibited by a variety of growth and survival factors, which induce BAD phosphorylation at the regulatory serines (Ser112, Ser136, and Ser155) and Thr201 (Danial and Korsmeyer, 2004; Danial, 2008; Dragovich et al., 1998; Liu and Lin, 2007; Youle and Strasser, 2008). Our results show that, unlike known BAD kinases, IKK phosphorylated BAD at Ser26 residue in vitro and in vivo (Figures 3 and 4). The phosphorylation most likely occurred in the cytoplasm, as both Ser26-phosphorylated BAD and IKKβ exclusively resided in the cytoplasm in WT fibroblasts (Figure 5A), and only non-Ser26-phosphorylated BAD translocated to the mitochondria in *Ikk*β$^{-/-}$ MEFs (Figure 5C). Thus, like survival factors, the inflammatory cytokine TNFα also inhibits BAD to suppress apoptosis.

Phosphorylation by IKK at Ser26 primes BAD for inactivation. Previously, it has been reported that phosphorylation of Ser112 and Ser136 is required for phosphorylation of Ser155, although the mechanism is still not known (Danial, 2008). Our results show that phosphorylation of BAD by IKK at Ser26 prevented BAD from translocating to the mitochondria (Figure 5A) by promoting the interaction between BAD with 14-3-3 (Figure 5B) and by suppressing the interaction between BAD with BCL-X_L (Figure 5C). Because the surrounding amino acids of Ser26 (DPGIRpSLG) do not comprise the 14-3-3 binding motif (typically RSXpS/TXP or RXXXXpS/TXP; Yaffe, 2002), IKK is most likely to regulate the association of BAD with 14-3-3 indirectly. In support of this notion, our data show that phosphorylation of BAD at the regulatory serines was impaired in *Ikk*β$^{-/-}$ MEFs (Figure 6A) and *Bad*$^{-/-}$ MEFs expressing BAD(S26A) mutant (Figure S6A). Thus,

phosphorylation of BAD by IKK at Ser26 is a prerequisition for BAD to be further phosphorylated at the regulatory serines. The Ser26-phosphorylated BAD(3SA) mutant still translocated to the mitochondria to induce apoptosis in TNFα-treated *Bad*(3SA)$^+$ MEFs (Figures 6B–6D), suggesting that Ser26-phosphorylation indeed depends on phosphorylation of the regulatory serines to exert its function. The percentage of Ser26-phosphorylated BAD(3SA) mutant is similar to that of BAD(3SA) mutant (Figure 6C) or BAD (Figure 5A) that translocates to the mitochondria in the early time period after TNFα stimulation (≤2 hr), indicating that phosphorylation of BAD by IKK at Ser26 plays a critical role in inhibiting the initiation of BAD mitochondrial translocation, thereby suppressing its proapoptotic activity. Future structural studies are needed to determine the mechanism underlying the priming effect of IKK-mediated Ser26 phosphorylation.

The inhibition of BAD by IKK is independent of NF-κB. Overwhelming evidence shows that IKK inhibits TNFα-induced apoptosis through activation of NF-κB (Baldwin, 2012; Ghosh and Karin, 2002; Karin and Ben-Neriah, 2000; Karin and Lin, 2002; Liu and Lin, 2007). Our results show that IKK directly phosphorylated BAD at Ser26, thereby inhibiting its proapoptotic activity upon TNFα stimulation (Figures 3, 4, 5, 6, and 7). This inhibition is independent of NF-κB, as BAD was still phosphorylated at Ser26 by IKK and was sequestered in the cytosol of *RelA*$^{-/-}$ MEFs (Figures 5D and 5E). Conversely, elimination of IKK-mediated BAD phosphorylation had no significant effects on RelA activation (Figures S6A and S6B). Although we cannot formally exclude that other IKK substrates might also be involved in regulation of TNFα-induced apoptosis, inactivation of BAD is an NF-κB-independent axis of the IKK survival signaling in suppression of TNFα-induced apoptosis.

The inactivation of BAD by IKK via Ser26 phosphorylation has physiological significance. Our results show that *Ikkβ*$^{-/-}$ MEFs died significantly faster than *RelA*$^{-/-}$/sicRel MEFs (Figures 1A–1C). This was due to lack of inhibition of BAD by IKK in *Ikkβ*$^{-/-}$ MEFs, as knockdown of BAD in *Ikkβ*$^{-/-}$ MEFs almost completely eliminated the difference (Figure 2C). Consistently, *Bad*(S26A)$^+$ MEFs died significantly faster than *Bad*(WT)$^+$ MEFs (Figures 7A–7C). More importantly, *Bad*(S26A)$^+$ mice had much earlier onset of liver damage with massive apoptosis of hepatocytes (Figure S6D) and died significantly faster than *Bad*(WT)$^+$ mice (Figure 7E). Thus, phosphorylation of BAD at Ser26 by IKK is a physiologically relevant and important regulation. This conclusion is further supported by the observations that similar results were obtained in *Bad*$^{3SA/3SA}$ knockin mice (Figures 6D, 6E, and S5B). Our findings are also consistent with previous reports that *Ikkβ*$^{-/-}$ mice died earlier (E13.5) (Li et al., 1999a, 1999b) than *RelA*$^{-/-}$ mice (E15–E16) (Beg et al., 1995). The inability of inactivating BAD in *Ikkβ*$^{-/-}$ mice might account for their earlier embryonic lethality. Future studies are needed to explore this scenario.

Inactivation of BAD by IKK may work in coordination with activation of NF-κB to inhibit TNFα-induced apoptosis. As a key survival factor, NF-κB is essential for cell survival upon TNFα stimulation. However, NF-κB activation is a relatively slow process that involves IκBα phosphorylation, ubiquitination, and degradation; nuclear translocation of NF-κB dimmer; induction of NF-κB target genes; and synthesis of corresponding protein products (Ghosh and Karin, 2002; Karin and Ben-Neriah, 2000). By contrast, inactivation of BAD by IKK is direct and rapid. Our results show that BAD was phosphorylated by IKK at Ser26 within minutes in TNFα-stimulated WT fibroblasts (Figures 4F, 6A, and S4). In the absence of IKKβ, BAD started to translocate to the mitochondria as early as 5 min after TNFα stimulation (Figure S4). It is most likely that BAD may be involved in the initiation of TNFα-induced apoptosis. The rapid inactivation of BAD by IKK may be critical to protect cells from TNFα-induced apoptosis before IKK-activated NF-κB is able to induce inhibitors of apoptosis (IAPs) to suppress the apoptosis. Thus, the two parallel and independent signaling axes of IKK (i.e., activation of NF-κB and inhibition of BAD) may function in coordination in inhibition of TNFα-induced apoptosis (Figure 7F).

EXPERIMENTAL PROCEDURES

Reagents

Antibodies against BAD, IκBα, PARP, phospho-IKKα/β, phospho-BAD(S112), phospho-BAD (S136), and phospho-BAD(S155) were from Cell Signaling. Anti-phospho-BAD(S26) antibody was custom made by Abiocode Inc. using the synthetic phosphopeptide RKSDPGIRpSLGSD as the immunogen. Antibodies against COX-II, BCL-X_L, IKKγ, RelA, cRel, pan 14-3-3, and Casp-3 were from Santa Cruz. Antibody against IKKβ was from Millipore. Anti-M2 antibody, the IKKβ inhibitor PS-1145, and Hoechst were from Sigma. Propidium iodide (PI) and Annexin V were from BD PharMingen. D-Galactosamine Hydrochloride (D-GalN) was from MP Biomedicals. [^{32}P]ATP was from PerkinElmer. TNFα was from R&D (murine) or PeproTech (human). pcDNA3.1-Hygromycin(+) vectors encoding M2-BAD or M2-BAD(S26A) mutant were subcloned, as described previously (Yu et al., 2004). S26A mutation and 3SA mutation were introduced using Quick-Change site-directed mutagenesis kit (Stratagene) and were verified by DNA sequencing. Expression vectors encoding HA-BCL-X_L, GST-BAD, GST-c-Jun, GST-IκBα, GST-ΔN-BAD(115–204), and GST-ΔC-BAD(1–114) were described previously (Yu et al., 2004). HA-IKKβ, HA-IKKβ(EE), and NF-κB luciferase reporter gene were gifts from Dr. Joseph A. DiDonato at Cleveland Clinic Foundation. IKKβ(EE) protein, which had been purified to near homogeneity from baculovirus-encoding IKKβ(EE)-infected sf9 cells, was a gift from Dr. Frank Muricio at Cellgene. The sequences of siRNA are siBAD: AGCUCCUGUUUGGAGUUUCAAA, siIKKβ: CAGAA GAGCGAAGUGG ACAUCU, siRelA: GAGUUUCAGCAGCUCCUGAAC, and siCtrl: GGAGCGCACCAUCUUCUUC. The recombinant adenovirus encoding WT *Bad*, *Bad*(S26A), or *Bad*(3SA) mutant or the EGFP control were generated using standard procedures and were purified by CsCl density gradient centrifugation (Xiang et al., 2000).

Cell Culture and Transfection

WT, *Ikkβ*$^{-/-}$, and *RelA*$^{-/-}$ MEFs and CHO cells were gifts from Dr. Michael Karin at University of California, San Diego. *Bad*$^{-/-}$ MEFs were described previously (Ranger et al., 2003). FL83B cells were from ATCC. Cells were grown in Dulbecco's modified Eagle's medium supplemented with 10% fetal bovine serum, 2 mM glutamine, 100 U/ml penicillin, and 100 μg/ml streptomycin. To establish *Bad*$^{-/-}$ MEFs stably expressing WT BAD or BAD(S26A) mutant, *Bad*$^{-/-}$ MEFs were first transfected with pcDNA3.1-Puromycin(+)-HA-BCL-X_L and selected with puromycin (1.5 μg/ml). *Bad*$^{-/-}$ MEFs stably expressing HA-BCL-X_L were then transfected with pcDNA3.1-Hygromycin(+)-M2-BAD or -M2-BAD(S26A) and were further selected with hygromycin (100 μg/ml).

Animal Experiments

Bad$^{-/-}$ and *Bad*$^{3SA/3SA}$ mice were described previously (Danial, 2008). *Bad*$^{-/-}$ mice were injected through tail vein with recombinant adenoviral vector encoding *Bad*(WT) or *Bad*(S26A) mutant (a total dose of 4 × 10^9 infectious units

per ml [IFUs] in a volume of 100 μl per animal) to generate *Bad*(WT)$^{+}$ and *Bad*(S26A)$^{+}$ mice, respectively.

To determine the role of IKK-mediated phosphorylation and inactivation of BAD in TNFα-apoptosis in vivo, WT, *Bad*$^{-/-}$, *Bad*$^{3SA/3SA}$ knockin, and various reconstituted *Bad*$^{-/-}$ mice (6–8 weeks old, 20–24 g) were sensitized by i.p. administration of 700 mg/kg body weight of D-GalN and then treated with i.p. administration of 15 μg/kg body weight of hTNFα. All reagents were balanced with sterile PBS so that the total volume of injecting solution in different mice was the same. Mortality rate was recorded every 2 hr for up to 25 hr after the treatment. The animal protocols were approved by University of Chicago Institutional Animal Care and Use Committee. To analyze liver injury, livers were isolated from premoved mice, and the liver lobes were excised and fixed in 4% paraformaldehyde for 12 hr. The tissues were sliced to 5 μm thickness. H&E staining was performed at the University of Chicago Human Tissue Resource Center (HTRC). In situ cell death was analyzed by TUNEL staining (TUNEL Apoptosis Detection kit, EMD Millipore) according to the manufacturer's protocol.

Statistical Analysis

The percentage of apoptotic cells among groups was determined using Student's t test. Mouse survival curves were constructed using the Kaplan-Meier product limit estimator and compared using the log rank (Mantel-Cox) test. $p < 0.05$ was considered to be significant in all experiments.

SUPPLEMENTAL INFORMATION

Supplemental Information includes Extended Experimental Procedures and six figures and can be found with this article online at http://dx.doi.org/10.1016/j.cell.2012.12.021.

ACKNOWLEDGMENTS

We are grateful to Drs. David A. Brenner, Joseph A. DiDonato, Michael Karin, Stanley Korsmeyer, and Frank Mercurio for reagents that make this work possible. This work is partially supported by National Basic Research Program of China (2012CB910801), National Natural Science Foundation of China (31130035), Chinese Academy of Sciences (SIBS2010CSP001), and National Institutes of Health grants CA100460 (to A.L.), CA128114 (to J.X.), and GM081603 (to J.L.).

Received: May 22, 2012
Revised: October 2, 2012
Accepted: December 13, 2012
Published: January 17, 2013

REFERENCES

Alcamo, E., Mizgerd, J.P., Horwitz, B.H., Bronson, R., Beg, A.A., Scott, M., Doerschuk, C.M., Hynes, R.O., and Baltimore, D. (2001). Targeted mutation of TNF receptor I rescues the RelA-deficient mouse and reveals a critical role for NF-κB in leukocyte recruitment. J. Immunol. *167*, 1592–1600.

Anest, V., Hanson, J.L., Cogswell, P.C., Steinbrecher, K.A., Strahl, B.D., and Baldwin, A.S. (2003). A nucleosomal function for IkappaB kinase-α in NF-kappaB-dependent gene expression. Nature *423*, 659–663.

Baldwin, A.S. (2012). Regulation of cell death and autophagy by IKK and NF-κB: critical mechanisms in immune function and cancer. Immunol. Rev. *246*, 327–345.

Barkett, M., and Gilmore, T.D. (1999). Control of apoptosis by Rel/NF-kappaB transcription factors. Oncogene *18*, 6910–6924.

Baud, V., and Karin, M. (2001). Signal transduction by tumor necrosis factor and its relatives. Trends Cell Biol. *11*, 372–377.

Beg, A.A., Sha, W.C., Bronson, R.T., Ghosh, S., and Baltimore, D. (1995). Embryonic lethality and liver degeneration in mice lacking the RelA component of NF-κB. Nature *376*, 167–170.

Bonni, A., Brunet, A., West, A.E., Datta, S.R., Takasu, M.A., and Greenberg, M.E. (1999). Cell survival promoted by the Ras-MAPK signaling pathway by transcription-dependent and -independent mechanisms. Science *286*, 1358–1362.

Comb, W.C., Hutti, J.E., Cogswell, P., Cantley, L.C., and Baldwin, A.S. (2012). p85α SH2 domain phosphorylation by IKK promotes feedback inhibition of PI3K and Akt in response to cellular starvation. Mol. Cell *45*, 719–730.

Danial, N.N. (2008). BAD: undertaker by night, candyman by day. Oncogene *27* (*Suppl 1*), S53–S70.

Danial, N.N., and Korsmeyer, S.J. (2004). Cell death: critical control points. Cell *116*, 205–219.

Datta, S.R., Dudek, H., Tao, X., Masters, S., Fu, H.A., Gotoh, Y., and Greenberg, M.E. (1997). Akt phosphorylation of BAD couples survival signals to the cell-intrinsic death machinery. Cell *91*, 231–241.

del Peso, L., González-García, M., Page, C., Herrera, R., and Nuñez, G. (1997). Interleukin-3-induced phosphorylation of BAD through the protein kinase Akt. Science *278*, 687–689.

Dragovich, T., Rudin, C.M., and Thompson, C.B. (1998). Signal transduction pathways that regulate cell survival and cell death. Oncogene *17*, 3207–3213.

Gerondakis, S., Grossmann, M., Nakamura, Y., Pohl, T., and Grumont, R. (1999). Genetic approaches in mice to understand Rel/NF-kappaB and IkappaB function: transgenics and knockouts. Oncogene *18*, 6888–6895.

Ghosh, S., and Karin, M. (2002). Missing pieces in the NF-kappaB puzzle. Cell Suppl. *109*, S81–S96.

Grossmann, M., Metcalf, D., Merryfull, J., Beg, A., Baltimore, D., and Gerondakis, S. (1999). The combined absence of the transcription factors Rel and RelA leads to multiple hemopoietic cell defects. Proc. Natl. Acad. Sci. USA *96*, 11848–11853.

Harada, H., Becknell, B., Wilm, M., Mann, M., Huang, L.J.S., Taylor, S.S., Scott, J.D., and Korsmeyer, S.J. (1999). Phosphorylation and inactivation of BAD by mitochondria-anchored protein kinase A. Mol. Cell *3*, 413–422.

Hoffmann, A., and Baltimore, D. (2006). Circuitry of nuclear factor kappaB signaling. Immunol. Rev. *210*, 171–186.

Hu, M.C.T., Lee, D.F., Xia, W.Y., Golfman, L.S., Ou-Yang, F., Yang, J.Y., Zou, Y.Y., Bao, S.L., Hanada, N., Saso, H., et al. (2004). IkappaB kinase promotes tumorigenesis through inhibition of forkhead FOXO3a. Cell *117*, 225–237.

Hutti, J.E., Turk, B.E., Asara, J.M., Ma, A., Cantley, L.C., and Abbott, D.W. (2007). IkappaB kinase β phosphorylates the K63 deubiquitinase A20 to cause feedback inhibition of the NF-kappaB pathway. Mol. Cell. Biol. *27*, 7451–7461.

Karin, M., and Ben-Neriah, Y. (2000). Phosphorylation meets ubiquitination: the control of NF-[κ]B activity. Annu. Rev. Immunol. *18*, 621–663.

Karin, M., and Lin, A. (2002). NF-kappaB at the crossroads of life and death. Nat. Immunol. *3*, 221–227.

Kelekar, A., Chang, B.S., Harlan, J.E., Fesik, S.W., and Thompson, C.B. (1997). Bad is a BH3 domain-containing protein that forms an inactivating dimer with Bcl-XL. Mol. Cell. Biol. *17*, 7040–7046.

Li, Q.T., Van Antwerp, D., Mercurio, F., Lee, K.F., and Verma, I.M. (1999a). Severe liver degeneration in mice lacking the IkappaB kinase 2 gene. Science *284*, 321–325.

Li, Z.W., Chu, W.M., Hu, Y.L., Delhase, M., Deerinck, T., Ellisman, M., Johnson, R., and Karin, M. (1999b). The IKKbeta subunit of IkappaB kinase (IKK) is essential for nuclear factor kappaB activation and prevention of apoptosis. J. Exp. Med. *189*, 1839–1845.

Lin, A., Frost, J., Deng, T.L., Smeal, T., al-Alawi, N., Kikkawa, U., Hunter, T., Brenner, D., and Karin, M. (1992). Casein kinase II is a negative regulator of c-Jun DNA binding and AP-1 activity. Cell *70*, 777–789.

Liu, J., and Lin, A. (2007). Wiring the cell signaling circuitry by the NF-κB and JNK1 crosstalk and its applications in human diseases. Oncogene *26*, 3267–3278.

Liu, Z.G., Hsu, H.L., Goeddel, D.V., and Karin, M. (1996). Dissection of TNF receptor 1 effector functions: JNK activation is not linked to apoptosis while NF-kappaB activation prevents cell death. Cell *87*, 565–576.

Liu, J., Minemoto, Y., and Lin, A. (2004). c-Jun N-terminal protein kinase 1 (JNK1), but not JNK2, is essential for tumor necrosis factor α-induced c-Jun kinase activation and apoptosis. Mol. Cell. Biol. *24*, 10844–10856.

Liu, F., Xia, Y.F., Parker, A.S., and Verma, I.M. (2012). IKK biology. Immunol. Rev. *246*, 239–253.

Mercurio, F., Zhu, H.Y., Murray, B.W., Shevchenko, A., Bennett, B.L., Li, J.W., Young, D.B., Barbosa, M., Mann, M., Manning, A., and Rao, A. (1997). IKK-1 and IKK-2: cytokine-activated IkappaB kinases essential for NF-kappaB activation. Science *278*, 860–866.

Ranger, A.M., Zha, J.P., Harada, H., Datta, S.R., Danial, N.N., Gilmore, A.P., Kutok, J.L., Le Beau, M.M., Greenberg, M.E., and Korsmeyer, S.J. (2003). Bad-deficient mice develop diffuse large B cell lymphoma. Proc. Natl. Acad. Sci. USA *100*, 9324–9329.

Reiley, W., Zhang, M.Y., Wu, X.F., Granger, E., and Sun, S.C. (2005). Regulation of the deubiquitinating enzyme CYLD by IkappaB kinase γ-dependent phosphorylation. Mol. Cell. Biol. *25*, 3886–3895.

Rudolph, D., Yeh, W.C., Wakeham, A., Rudolph, B., Nallainathan, D., Potter, J., Elia, A.J., and Mak, T.W. (2000). Severe liver degeneration and lack of NF-kappaB activation in NEMO/IKKgamma-deficient mice. Genes Dev. *14*, 854–862.

Sakurai, H., Chiba, H., Miyoshi, H., Sugita, T., and Toriumi, W. (1999). IkappaB kinases phosphorylate NF-kappaB p65 subunit on serine 536 in the transactivation domain. J. Biol. Chem. *274*, 30353–30356.

Tang, G.L., Minemoto, Y., Dibling, B., Purcell, N.H., Li, Z.W., Karin, M., and Lin, A. (2001). Inhibition of JNK activation through NF-kappaB target genes. Nature *414*, 313–317.

Tang, F., Tang, G., Xiang, J., Dai, Q., Rosner, M.R., and Lin, A. (2002). The absence of NF-kappaB-mediated inhibition of c-Jun N-terminal kinase activation contributes to tumor necrosis factor α-induced apoptosis. Mol. Cell. Biol. *22*, 8571–8579.

Van Antwerp, D.J., Martin, S.J., Kafri, T., Green, D.R., and Verma, I.M. (1996). Suppression of TNF-α-induced apoptosis by NF-kappaB. Science *274*, 787–789.

Wang, C.Y., Mayo, M.W., and Baldwin, A.S., Jr. (1996a). TNF- and cancer therapy-induced apoptosis: potentiation by inhibition of NF-kappaB. Science *274*, 784–787.

Wang, H.G., Rapp, U.R., and Reed, J.C. (1996b). Bcl-2 targets the protein kinase Raf-1 to mitochondria. Cell *87*, 629–638.

Wegener, E., Oeckinghaus, A., Papadopoulou, N., Lavitas, L., Schmidt-Supprian, M., Ferch, U., Mak, T.W., Ruland, J., Heissmeyer, V., and Krappmann, D. (2006). Essential role for IkappaB kinase β in remodeling Carma1-Bcl10-Malt1 complexes upon T cell activation. Mol. Cell *23*, 13–23.

Xiang, J., Gómez-Navarro, J., Arafat, W., Liu, B., Barker, S.D., Alvarez, R.D., Siegal, G.P., and Curiel, D.T. (2000). Pro-apoptotic treatment with an adenovirus encoding Bax enhances the effect of chemotherapy in ovarian cancer. J. Gene Med. *2*, 97–106.

Yaffe, M.B. (2002). How do 14-3-3 proteins work?— Gatekeeper phosphorylation and the molecular anvil hypothesis. FEBS Lett. *513*, 53–57.

Youle, R.J., and Strasser, A. (2008). The BCL-2 protein family: opposing activities that mediate cell death. Nat. Rev. Mol. Cell Biol. *9*, 47–59.

Yu, C.F., Minemoto, Y., Zhang, J.Y., Liu, J., Tang, F.M., Bui, T.N., Xiang, J.L., and Lin, A. (2004). JNK suppresses apoptosis via phosphorylation of the pro-apoptotic Bcl-2 family protein BAD. Mol. Cell *13*, 329–340.

Zandi, E., Rothwarf, D.M., Delhase, M., Hayakawa, M., and Karin, M. (1997). The IkappaB kinase complex (IKK) contains two kinase subunits, IKKalpha and IKKbeta, necessary for IkappaB phosphorylation and NF-kappaB activation. Cell *91*, 243–252.

Zha, J.P., Harada, H., Yang, E., Jockel, J., and Korsmeyer, S.J. (1996). Serine phosphorylation of death agonist BAD in response to survival factor results in binding to 14-3-3 not BCL-X(L). Cell *87*, 619–628.